Electrodynamic Behaviour of the LHC Superconducting Magnet String during a Discharge

L. Coull, D. Hagedorn, G. Krainz, F. Rodriguez-Mateos, R. Schmidt, CERN, Geneva, Switzerland

Abstract

A string of three dipole magnets and one quadrupole magnet, representing a half cell of the future LHC collider, has been assembled and tested at CERN. In order to avoid high temperatures in the magnets and high voltages between coils and ground in case of a quench, a reliable magnet protection system is necessary. The magnets are by-passed by protection diodes which are located in the cold mass. In case of a quench most of the stored magnetic energy is dissipated in the resistive parts of the magnets. Many natural and heater provoked quenches have been performed during the two experimental runs of the string at 1.9 K. This paper describes the electrodynamic behaviour during a fast discharge (i.e. after a quench) of the magnet string configuration. A simulation program was developed to evaluate parameters which cannot be directly measured, such as the current sharing between magnets and diodes, as well as the dissipated energy. The simulation program gives also the possibility for worst-case calculations, for example non-uniform magnet quench characteristics and protection heater delays.

1 LHC MAGNET STRING

The present configuration of the magnet string includes one superconducting quadrupole LSQP and three superconducting bending dipole magnets MTP1A1 to MTP1A3, which are electrically connected in series. Table 1 shows the parameters of the quadrupole and dipoles relevant for this paper. The string is powered by a 20 kA, 14 V converter. External dump resistors in parallel to circuit breakers are installed [1].

When a quench occurs, the resistive voltage rise is detected by quench detectors. Quench heater strips are mounted on the outer layer coils of each magnet. When a quench is detected, capacitors are discharged through these quench heater strips. The cables which are in contact with the quench heater strips become normal conducting. The distribution of the stored energy over the whole length of a magnet avoids an excessive heating at the origin of the quench. At the same time as the heaters are fired, the power converter is switched off. The discharge current continues to flow across the free-wheeling diode in parallel to the power converter. During the discharge, diodes in the cold mass by-pass a part of the current and thus limit the voltages across the magnets to the diode forward voltages.

	unit	Quadrupole	Dipoles
Magnet parameters:			
Inductance	mH	8	58
Magnetic length	m	3.1	9
Operation current	A	12400	12400
Cable parameters:			
met. cross sect.(o.l.)	mm^2	22.4	34.0
met. cross sect.(i.l.)	mm^2	22.4	22.2
Ratio Cu/SC		1.8	1.8
RRR		94	82-112

Table 1: Magnet parameters for quadrupole and dipoles

2 ELECTRODYNAMIC BEHAVIOUR

The model for simulating the electrodynamic behaviour is based on a simplified network scheme of the LHC magnet string (Fig. 1). Each magnet is represented by the self in-

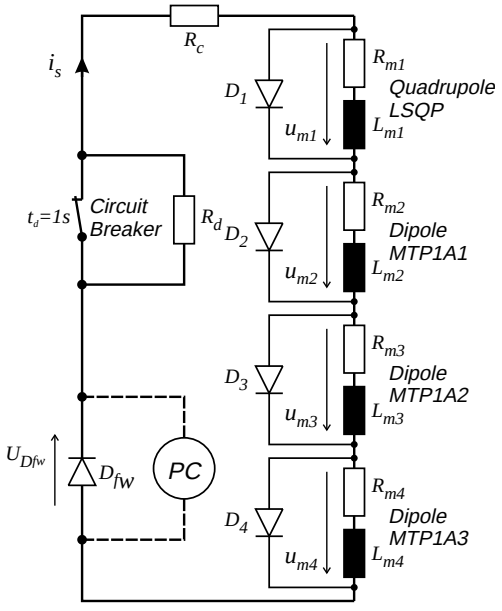

Figure 1: Electric scheme of the superconducting magnet string configuration

ductance L_m and the coil resistance R_m. The indices 1 to 4 correspond to the location of the magnets in the string, where the first magnet is the quadrupole followed by the three dipole magnets. The model solves the electrical net-

work equation

$$U_{Dfw} + (R_d + R_c)\, i_s + \sum_{k=1}^{N} u_{mk} = 0$$

with i_s the main current through the magnet string, U_{Dfw} the voltage across the free-wheeling diode in parallel to the power converter, u_{mk} the voltage across the $k-th$ magnet, R_d the dump resistor in parallel to the circuit breaker, R_c the resistance of the water cooled cables outside the magnet string, and N the number of magnets. Coil capacities and bus-bar inductances are not taken into account for the development of the model.

As long as the voltage across a magnet u_m is below the turn-on voltage of the by-passing diode U_f, the whole decay current i_s flows through this magnet. If u_m becomes equal to U_f, then the diode starts conducting in order to clamp the magnet voltage. The current i_s decays according to the equation

$$i_s = \left(I_0 + \frac{U_{Dfw} + U_k}{R_e + R_j}\right) e^{-\frac{R_e + R_j}{L_j} t} - \frac{U_{Dfw} + U_k}{R_e + R_j}$$

with $R_e = R_c + R_d$ the external resistance, $R_j = \sum_j R_{mj}$ the coil resistance and $L_j = \sum_j L_{mj}$ the inductance of the magnets where u_m is below U_f, $U_k = \sum_k U_{fk}$ the sum of u_m for the magnets which have already reached the turn-on voltage levels of the by-passing diodes, and I_0 the initial current before the decay. Due to the by-pass diode circuit, i_s splits up into a magnet current i_m and a diode current i_d (Fig. 2). The current decay in a single magnet can be de-

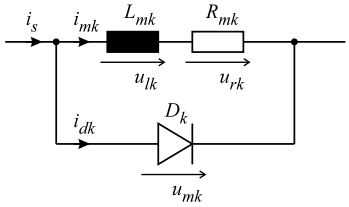

Figure 2: Magnet with cold diode by-pass

duced from the differential equation

$$u_m = R_m \cdot i_m + L_m \cdot \frac{di_m}{dt}$$

which gives

$$i_m = \frac{U_m}{R_m}\left(1 - e^{-\frac{R_m}{L_m} t}\right) + I_0 \cdot e^{-\frac{R_m}{L_m} t}.$$

With use of Kirchhoff's first law, the current through the by-passing diode is

$$i_d = i_s - i_m.$$

The forward voltage of the by-pass diode is a non linear function of temperature below 80 K. It depends also on the current. A satisfying approximation is given with the fit-function

$$U_f = \sum_{n=1}^{3} (a_n + b_n \cdot i_d) \cdot e^{-(c_n + d_n \cdot i_d) \cdot dT_d},$$

where a_n, b_n, c_n, and d_n are the diode dependent fit parameters.

The dissipated energy in a magnet is calculated by

$$W_m = \int_{t=0}^{\infty} {i_m}^2 \cdot R_m \cdot dt.$$

Above 10 K the cable resistance R_m is a non linear function of temperature. In the adiabatic approximation the temperature rise of a conductor carrying a current is governed by the heat balance [2]

$$i_m^2 \frac{\rho_{Cu}}{A_{Cu}} dt = \left(\delta_{Cu} \cdot A_{Cu} \cdot c_{pCu} + \delta_{SC} \cdot A_{SC} \cdot c_{pSC}\right) dT$$

$\rho_{Cu} = \rho_{Cu}(B, T, RRR)$, $c_{pCu} = c_{pCu}(T)$, $c_{pSC} = c_{pSC}(T)$, with c_{pCu} and c_{pSC} the heat capacity, A_{Cu} and A_{SC} the cross section, δ_{Cu} and δ_{SC} the density of copper and NbTi, ρ_{Cu} the electric resistivity of copper, and RRR is the residual resistivity ratio of copper.

From the heat balance equation, the average temperature in the normal conducting part of a magnet coil can be calculated by solving the integral

$$T = \int_{t=0}^{\infty} \frac{i_m^2 \cdot \rho_{Cu} \cdot dt}{A_{Cu} \cdot (A_{Cu} \cdot \delta_{Cu} \cdot c_{pCu} + A_{SC} \cdot \delta_{SC} \cdot c_{pSC})}.$$

Due to the nonlinear functions of heat capacity c_p, electric resistivity ρ, and diode forward voltage U_f, a numerical simulation program, written in MATLAB [3], solves the equations in an iterative way. This is an useful tool to analyse the electrodynamic behaviour by deducing parameters, which cannot be directly measured. With some input parameters from experiments, such as initial current and differences in heater delays, the program calculates the current sharing between magnets and by-pass diodes, the voltages across magnet apertures, the average coil temperatures, and the dissipated energy in the different magnets.

3 RESULTS

Many of the experiments on the LHC magnet string were performed by firing the quench heaters in all magnets at the same time. On the assumption that all dipoles have identical behaviour, after firing the quench heaters, no current would flow across the by-passing diodes. But in reality differences in constructions and in material properties lead to specific effects in each magnet. Mainly the quench heater delay and RRR are responsible for the different characteristics in the development of resistive voltage. In magnet coils with high RRR values, the resistive voltage rises up slower than in coils with lower RRR values. The heater delay time depends for these tests on the current level.

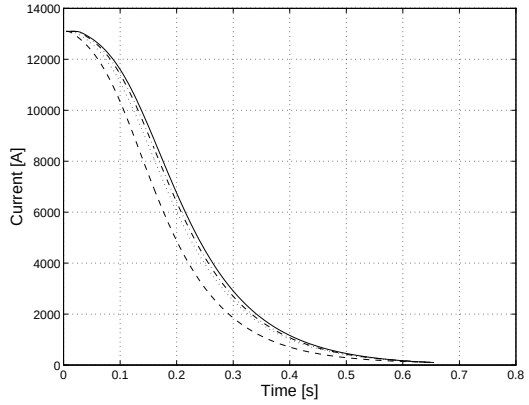

Figure 3: Deduced magnet currents during a fast discharge from 13.1 kA: LSQP (dashed line), MTP1A1 (solid line), MTP1A2 (dashdot line), MTP1A3 (dotted line)

Since superconducting magnets in the string do not all have the same quench behaviour, the current sharing between magnets and diodes is different (Fig. 3). The part of the string current which flows during the discharge through the by-pass diodes is shown in Fig. 4. Dipole MTP1A1 is the magnet with the highest RRR value. The resistive voltage in all the other magnets rises faster than in MTP1A1, but the heater delay in this magnet is rather low. This causes voltage jumps at the beginning of the discharge (Fig. 5). After about

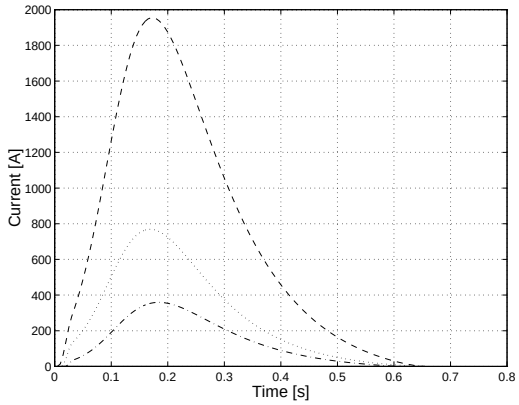

Figure 4: Deduced by-pass diode currents during a fast discharge from 13.1 kA

30 ms the inductive voltage in MTP1A1 blocks the corresponding by-pass diode. The magnet voltage of MTP1A1 then remains negative (Fig. 5). The voltages across single apertures in a magnet are usually higher than the total magnet voltage, because of the difference of RRR and heater delay between apertures. The difference in heater delay between dipole apertures is within the same range for all dipoles in the LHC magnet string. Since the difference in RRR between apertures in dipole MTP1A2 is higher than in the other magnets, the aperture voltages rise up to more than hundred volts during the discharge after a quench at high current (Fig. 6). They are acceptable and do not endanger

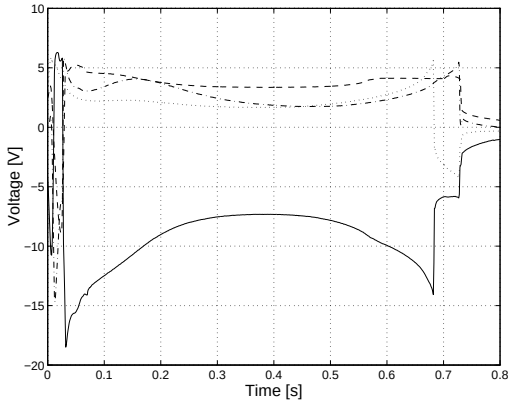

Figure 5: Measured magnet voltages during a fast discharge from 13.1 kA

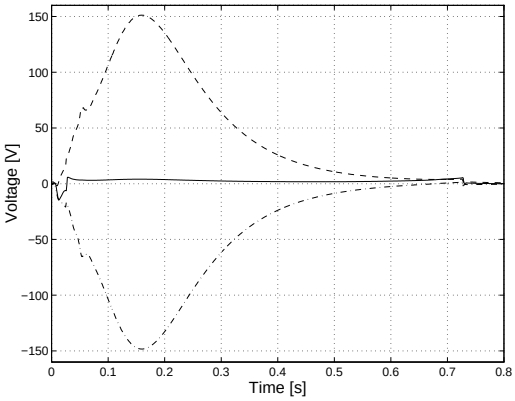

Figure 6: Measured aperture voltages during a fast discharge from 13.1 kA in MTP1A2

the LHC magnet string. Simulations have shown that the average coil temperatures in a dipole after a quench from high current is in the range of 200 K.

4 CONCLUSIONS

The analysis of the electrodynamic behaviour in the LHC magnet string shows that in the present configuration all parameters are within the specified limits. Simulations show that the effect of different RRR between the apertures of a dipole is rather small in comparison to the influence of quench heater delays between apertures. By changing the input parameters, the simulation program can be also easily adapted to modified magnet string configurations.

5 REFERENCES

[1] F.Rodriguez-Mateos et al., Electrical Performance of a String of Magnets Representing a Half Cell of the LHC Machine, Tampere, 1995

[2] M.S. McAshan, MIITs Integrals for Copper and for Nb-46.5 wt% Ti, SSC-N-468, 1988

[3] Numerical Analysis and Data Processing Software Package, The MathWorks Inc., 1995